

Ultrafast optical modulators based on the nonlinear optical response of an electron–hole plasma

M.V. Ermolenko, V.V. Stankevich, O.V. Buganov, S.A. Tikhomirov,
S.V. Gaponenko, P.I. Kuznetsov, G.G. Yakusheva

Abstract. The nonlinear optical properties of multilayer heterostructures based on zinc chalcogenides are studied. Rapid variations in the reflection and transmission of samples excited by ultrashort laser pulses are demonstrated. The characteristic relaxation times of the induced nonlinearity are 2–5 ps and are almost independent within the experimental error on the excitation energy and temperature of a sample.

Keywords: ultrafast optical modulators, multilayer heterostructures, electron-hole plasma.

1. Introduction

All-optical and electrooptical modulators are indispensable elements of integrated electrooptical circuits. A great number of various types of ultrafast modulators have been proposed [1–9], but many of them have either large size [10, 11] or too complex [12–15], which impedes technologically their integration. The use of LiNbO₃ crystals, which are widely employed in fibreoptic communication lines [14], is hindered due to technological complications in their matching with semiconductors in integrated chips.

At present devices based on semiconductor optical amplifiers belong to the fastest optical modulators [15]. However, to maintain the population inversion of carriers in such amplifiers, voltage should be applied constantly, which leads to the heating of a chip and increase the total energy consumption of the device.

In addition, the operation of many devices is limited by absorption induced by injected carriers [2, 16]. The total loss due to induced absorption and during coupling of radiation into miniature devices [12] strongly reduces the useful signal.

At this paper, we propose to control light fluxes by using nonlinear optical effects in periodic multilayer heterostruc-

tures (Bragg mirrors) caused by the generation of an electron–hole (e–h) plasma in one of the sublattices of semiconductor heterostructures upon laser excitation [17]. When the e–h plasma is generated in one of the sublattices, the refractive index in its transparency region strongly changes, while the second sublattice remains unexcited and absorption in both sublattices remains negligible. The change in the refractive index of one of the heterostructure sublattices causes the shift of reflection and transmission bands. By producing the population of free carriers at which their plasma frequency approaches the required spectral range and optimising the position of the band-gap edge of the photonic structure with respect to this range, we can modulate the reflection (transmission) coefficient of structures in the transparency region of semiconductors.

Materials for the fabrication of such heterostructures should satisfy the following conditions: they should have substantially different energies of band gaps and the minimal possible mismatch of lattice constants. We demonstrate the possibility of fabricating ultrafast optical modulators of this type based on ZnS/ZnSe heterostructures.

2. Optical response of the e–h plasma

Among a variety of nonlinear optical effects produced in semiconductors at high excitation levels, three main groups can be distinguished:

- (i) effects related to variations in the carrier concentration;
- (ii) nonlinearities caused by the generation of a dense e–h plasma and its subsequent cooling;
- (iii) higher-order nonlinear effects determined directly by the medium polarisation.

We will omit the latter group of effects, although they provide the shortest response times (comparable with the excitation pulse duration), because, as a rule, they can be obtained only in bulk materials by using complex resonators and (or) additional elements to control light beams. We will not consider the first group as well because the nonlinear response caused by the change in the carrier concentration is formed near the band-gap edge, and modulators based on this principle have the large absorption loss. In addition, the radiative recombination time in many materials amounts to a few nanoseconds. The nonradiative relaxation leads to the strong heating of a lattice and is considerable at high defect concentrations. The influence of Auger recombination is manifested at free carrier concentrations exceeding 10^{21}

M.V. Ermolenko, V.V. Stankevich, O.V. Buganov, S.A. Tikhomirov,
S.V. Gaponenko B.I. Stepanov Institute of Physics, National Academy
of Sciences of Belarus, prosp. Nezavisimosti 68, 220072 Minsk, Belarus;
e-mail: ermolenko@imaph.bas-net.by;

P.I. Kuznetsov, G.G. Yakusheva Institute of Radio Engineering and
Electronics, Russian Academy of Sciences, ul. Vvedenskogo 1, 141120
Fryazino, Moscow region, Russia

Received 23 January 2008; revision received 5 November 2008

Kvantovaya Elektronika 39 (4) 361–366 (2009)

Translated by M.N. Sapozhnikov

cm^{-3} . The carrier concentration cannot change rapidly (for times shorter than 1 ns) due to diffusion because of the low diffusion rate. We will consider the generation of the e–h plasma and effects accompanying its cooling as a method for controlling light fluxes. The advantage of these effects is that modulators based on them have weak absorption (induced absorption far from the absorption region is negligible) and the response rate of the modulator is independent of its operation temperature.

The main contribution to variations in the refractive index during the formation and cooling of the e–h plasma is produced by the e–h plasma itself, which has the intrinsic permittivity, and by the subsystem of optical phonons generated during plasma cooling. Because changes in the refractive index in both systems have opposite signs, its decrease caused by the e–h plasma is compensated by the generation of phonons, and since the phonon generation time is approximately equal to the plasma cooling time, the relaxation time should be a few picoseconds. Thus, the relaxation kinetics of induced variations in the transparency region of semiconductors can be determined significantly by processes caused by the e–h plasma cooling.

We studied this possibility by using ZnS/ZnSe Bragg structures produced by the MOCVD method. All the parameters of this pair of materials are suitable for manufacturing modulators: ZnS is transparent in the optical pump region, while the absorption coefficient of ZnSe is $\sim 10^4 \text{ cm}^{-1}$. The difference between the refractive indices of these materials is quite large (~ 0.3) along with a small mismatch between their lattice constants.

3. Experimental

The multilayer ZnSe/ZnS heterostructures under study were obtained by MOCVD from organoelemental compounds [18]. The heterostructures were grown in the $\text{Zn}(\text{C}_2\text{H}_5)_2$ – $(\text{CH}_3)_2\text{Se}$ – $(\text{C}_2\text{H}_5)_2\text{S}$ system at the hydrogen pressure close to the atmospheric pressure in a slit-like quartz reactor at temperatures 425–470 °C on substrates made of single-crystal gallium arsenide plates with the (100) orientation. Before growing, the oxide layer was removed by keeping the substrate for 5 min at 600 °C in a hydrogen flow. To exclude the production of defects due to the difference in the lattice constants of GaAs and ZnSe, the heterostructure was grown on a 105-nm-thick ZnSe buffer layer. With the flow rates of $\text{Zn}(\text{C}_2\text{H}_5)_2$, $(\text{CH}_3)_2\text{Se}$ and $(\text{C}_2\text{H}_5)_2\text{S}$ equal to 5.5, 10.4 and 11.8 $\mu\text{mol min}^{-1}$, respectively, the growth of single-crystal ZnSe and ZnS layers was provided in the chosen temperature interval. To produce a mirror-smooth surface, diethyl zinc was supplied into a reactor 1–2 s before the growth of each subsequent layer. The quality of heterostructures was estimated by photoluminescence and X-ray diffractometry, while their thickness was determined by ellipsometry and from reflection spectra. The thickness of layers was selected so that the reflection maximum of a Bragg mirror was located near the edge of the fundamental absorption band of ZnSe.

Nonlinear optical properties were studied by using a femtosecond spectrometer [19] based on an original femtosecond Ti:sapphire laser [20] synchronously pumped by a passively mode-locked, negative-feedback pulsed Nd:YAG laser, and on a regenerative amplifier. This system produces tunable 150-fs pulses with energy of up to 1 mJ and a pulse repetition rate of 10 Hz in the range from 760 to 820 nm.

Fundamental pulsed radiation at the amplifier output is split into two beams with the energy ratio 1 : 4. The more intense radiation beam or its harmonic after propagation through a tunable delay line is used for pumping. The pump power density in the sample region being probed was changed by the longitudinal displacement of a focusing lens. The induced nonlinearity was probed with a supercontinuum generated by focusing a weaker fundamental radiation beam to a 1-cm cell with water. The continuum radiation was split into two identical beams (reference and signal) in a beamsplitter, which were focused into a sample by mirrors. The reference pulse was incident on the sample before the arrival of the excitation pulse, while the signal pulse was delayed by the time Δt with respect to the excitation pulse. The spectra of both pulses were recorded during each laser pulse by using a polychromator equipped with a CCD array and a microprocessor.

Experiments were performed by using the first and second harmonics of a Ti:sapphire laser at 780 and 390 nm with pulsed energies 250 and 20 μJ , respectively.

4. Results and discussion

We studied the nonlinear optical properties of multilayer heterostructures consisting of thin selenide and zinc sulfide monolayers. Laser pulses excited the zinc selenide sublattice, which resulted in the change in the refractive index

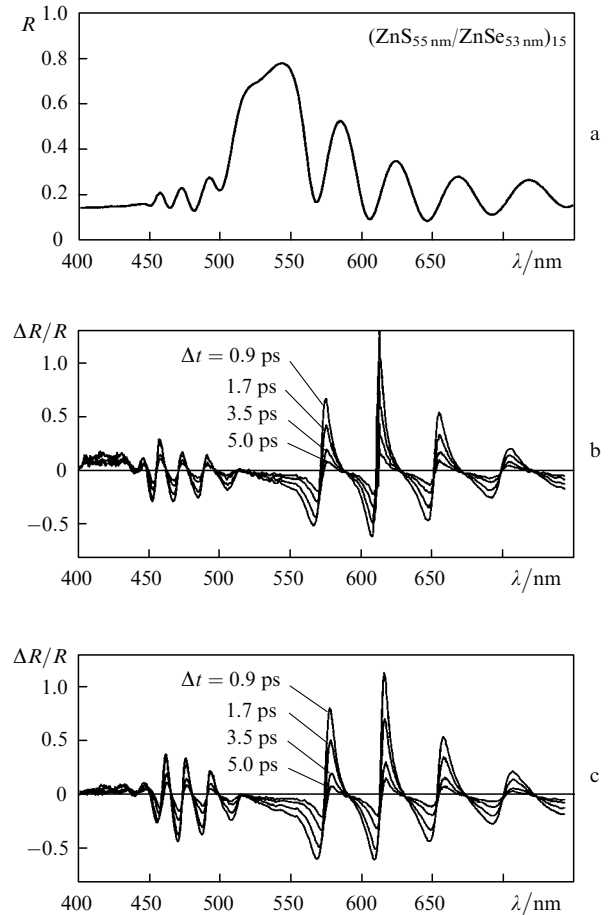


Figure 1. Reflection spectrum (a) and differential reflection spectra (b, c) of a multilayer heterostructure on a GaAs substrate excited by 150-fs, 390-nm laser pulses at 77 K (b) and 300 K (c) at different delays.

of this material. By modulating the refractive index in this way, we could dynamically control the optical properties of multilayer heterostructures.

We present the results obtained for multilayer structures consisting of 15 pairs of ZnSe/ZnS layers. The spectra were recorded in a broad wavelength range.

Figure 1 shows the ‘stationary’ room-temperature reflection spectrum of a sample consisting of 15 pairs of ZnS and ZnSe layers of thickness 55 and 53 nm, respectively, and also differential reflection spectra upon laser excitation of this heterostructure at two temperatures. Upon excitation of the

heterostructures, the reflection spectrum shifts to the blue due to the decrease in the refractive index of zinc selenide. Because the nonlinear response is mainly determined by the properties of the zinc selenide sublattice, it could be expected that the relaxation kinetics of the induced reflection of the structure change considerably with decreasing the sample temperature down to the liquid nitrogen temperature, because the band gap width, the shape of the absorption band-gap edge of zinc selenide and the efficiency of energy transfer from hot carriers to the lattice depend on temperature. However, the differential spectra (Figs 1b, c) and the relaxation kinetics of induced absorption (Fig. 2) are almost completely independent of temperature. Small variations in the spectra in the region 400–500 nm are explained by the temperature dependences of the shape and position of the absorption band-gap edge of ZnSe.

The independence of the shape and kinetics of differential reflection spectra from temperature suggests that the generation of polar optical phonons at the given excitation energy is almost independent of the crystal lattice temperature and that the nonlinear response is independent of the exciton subsystem (because the energy of lattice phonons at room temperature exceeds the exciton Rydberg, while at the liquid nitrogen temperature the phonon energy is smaller than the exciton Rydberg).

Figure 3 presents the induced-reflection kinetics at a wavelength of 526 nm for a sample consisting of 15 pairs of ZnS and ZnSe layers of thickness 65 and 46 nm, respectively, for different excitation energies. One can see that the measured nonlinearity relaxation time is almost independent of the excitation energy, and the nonlinear response saturates at the energy 15 μJ .

The independence of the measured relaxation times from the excitation pulse energy indicates that nonlinear effects related to the concentration of free carriers (induced recombination, Auger recombination, etc.) are not dominant in this case.

The removal of a gallium arsenide substrate eliminated its influence on the optical properties of the heterostructure, including the diffusion of carriers and energy transport to the substrate. In addition, the recording of transmission spectra gives additional information on nonlinear processes proceeding in multilayer heterostructures excited by intense laser radiation (Figs 4–7).

The differential transmission density spectra, apart from changes in the wide spectral range, exhibit a strong band at 450 nm caused by the change in the shape of the absorption band-gap edge of zinc selenide. Note that the relaxation time of induced absorption in this spectral region is approximately twice the relaxation time of the longer-wavelength spectral region (Fig. 5) and for samples on a GaAs substrate (Figs 2 and 3), which indicates different relative contributions of mechanisms responsible for the relaxation of induced absorption in different spectral regions.

Differences between ‘stationary’ and differential reflection spectra presented in Figs 1 and 6 are caused by the influence of the GaAs substrate on the reflection spectrum of the heterostructure due to additional Fresnel reflection at the GaAs–ZnSe interface. The time dependences of induced absorption in both cases give close values of the relaxation time constant.

We estimated changes in the refractive index of the heterostructure due to formation of a dense e–h plasma

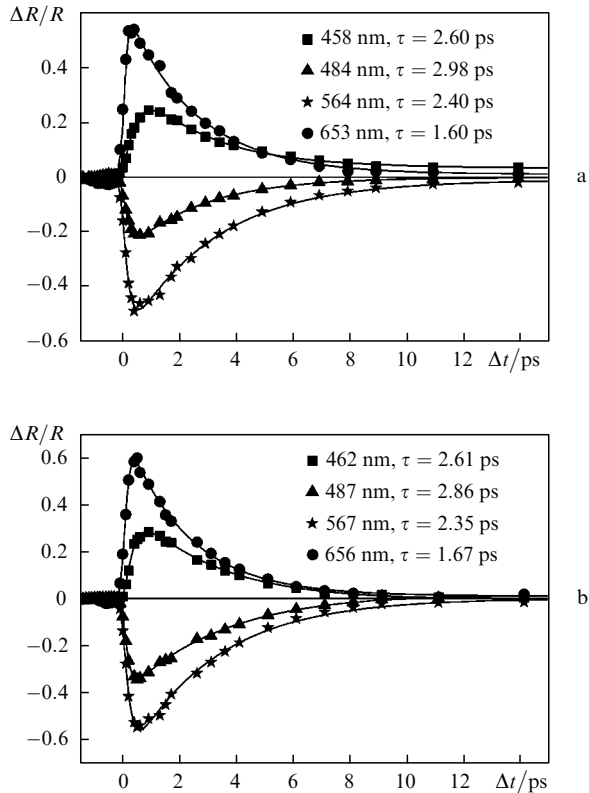


Figure 2. Relaxation kinetics of induced variations in reflection at different wavelengths for a multilayer heterostructure excited by 150-fs, 390-nm laser pulses at temperatures 77 K (a) and 300 K (b); τ is the relaxation time.

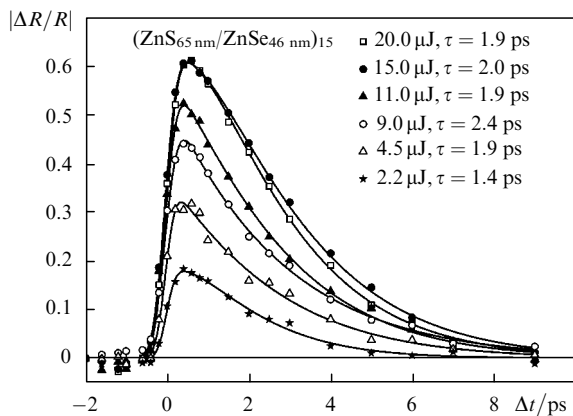


Figure 3. Relaxation kinetics of induced variations in reflection at 526 nm of a multilayer heterostructure excited by 150-fs, 390-nm pulses with different energies.

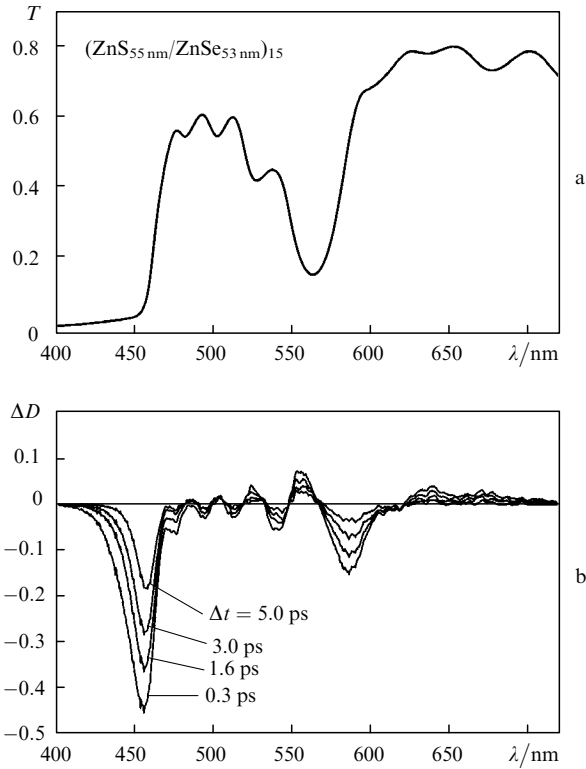


Figure 4. Transmission (a) and induced optical density (b) spectra of a multilayer heterostructure with a removed GaAs substrate excited by 150-fs, 390-nm laser pulses with different delays Δt .

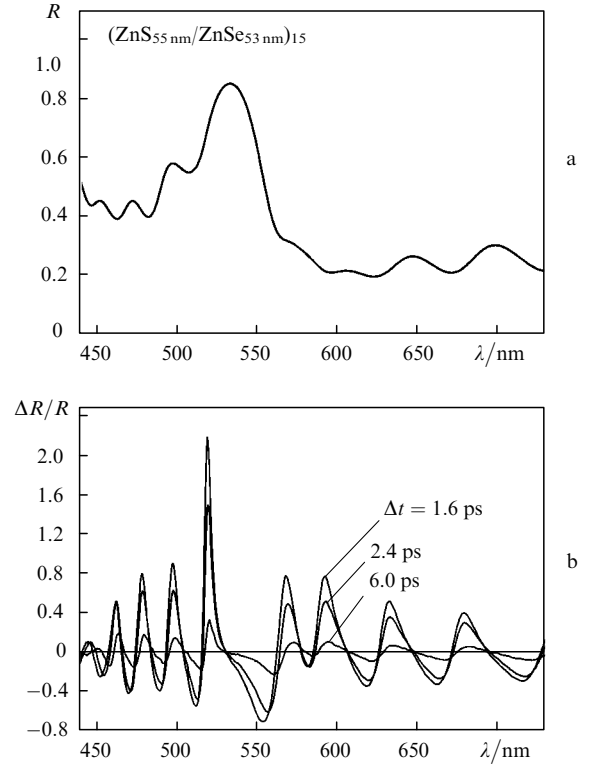


Figure 6. Reflection spectrum (a) and differential reflection spectra (b) of a multilayer structure with a removed GaAs substrate excited by 150-fs, 400-nm laser pulses with different delays Δt .

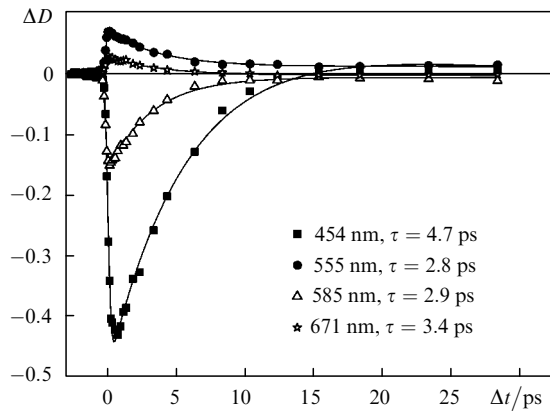


Figure 5. Relaxation kinetics of the induced optical density at different wavelengths in a multilayer heterostructure with a removed GaAs substrate excited by 150-fs, 390-nm laser pulses.

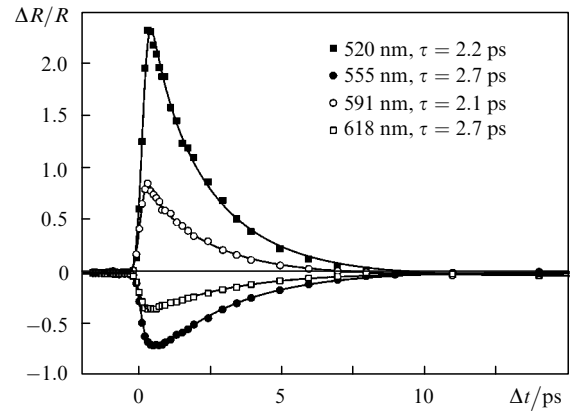


Figure 7. Relaxation kinetics of induced variations in reflection in a multilayer heterostructure with a removed GaAs substrate excited by 150-fs, 400-nm laser pulses.

($\sim 10^{19} \text{ cm}^{-3}$) with the cooling time $\sim 10^{-11} \text{ s}$ by using the expression [21]

$$\varepsilon = \varepsilon(0) + i\varepsilon'(0) - \frac{Nq^2}{\mu(\omega^2 + i\omega/\tau)} \equiv (n + ik)^2,$$

where $\varepsilon(0) + i\varepsilon'(0)$ is the permittivity in the absence of excitation; N is the carrier concentration; $q^2 = e^2/(4\pi\varepsilon_0)$; ε_0 is the electric constant; e is the electron charge; μ is the effective carrier mass; ω is the radiation frequency; and τ is the relaxation time.

Variations in the refractive index were also estimated from changes in the reflection spectra observed upon laser

excitation, which were simulated by the method of transmission matrices. Both these estimates give the refractive index change ~ -0.03 in the near-IR range.

A comparison of the spectra calculated within the framework of the dispersion model of the e-h plasma (Fig. 8) with experimental spectra (Fig. 1) shows good agreement between them in the transparency region of materials. The nonlinear response near the absorption band-gap edge is determined not only by the plasma contribution but also by other nonlinear processes (the energy band-gap renormalisation and screening of the Coulomb interaction between electrons and holes). Good agreement between experimental data and calculations allowed us to calculate a modulator, based on the principle

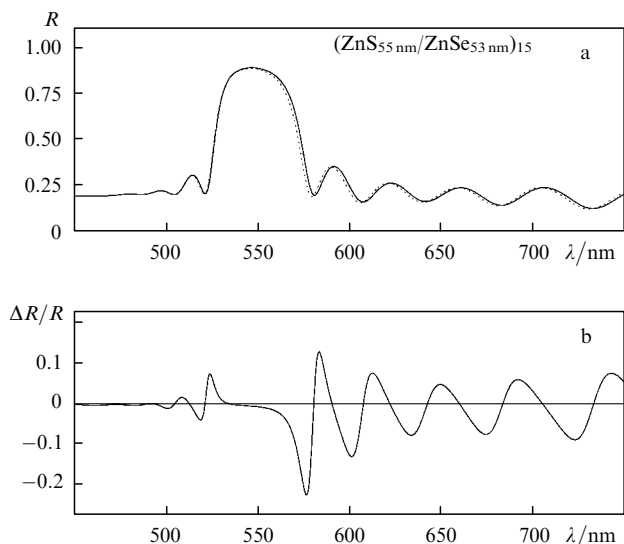


Figure 8. Calculated reflection spectrum with excitation (dotted curve) and without excitation (solid curve) (a) and the differential reflection spectrum (b) for a multilayer heterostructure on a GaAs substrate; $N = 3 \times 10^{19} \text{ cm}^{-3}$, $\tau = 10^{-11} \text{ s}$.

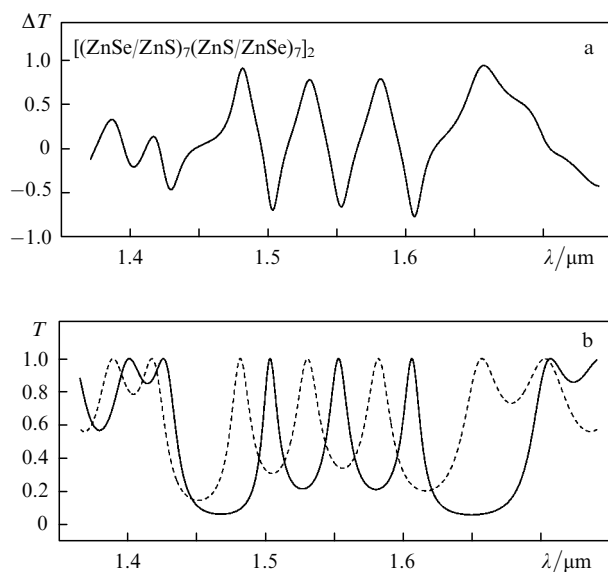


Figure 9. Differential transmission spectrum (a) and transmission spectra with excitation (dotted curve) and without excitation (solid curve) for the $[(\text{ZnSe}/\text{ZnS})_7(\text{ZnS}/\text{ZnSe})_7]_2$ model structure with 159-nm-thick ZnSe and 171-nm-thick ZnS layers; $N = 3 \times 10^{19} \text{ cm}^{-3}$, $\tau = 10^{-11} \text{ s}$.

described above, for the wavelength range from 1.5 to 1.6 μm used in fibreoptic communication lines. We performed a numerical experiment with parameters from previous experiments ($N \sim 10^{19} \text{ cm}^{-3}$ and $\tau \sim 10^{-11} \text{ s}$) by simulating the structure by a Bragg mirror with the reflection maximum at 1.55 μm and three symmetric defects (Fig. 9b). The simulation showed that the change in transmission close to 100% can be obtained already at the carrier concentration of $3 \times 10^{19} \text{ cm}^{-3}$ (Fig. 9a), the change in the refractive index being ~ -0.08 and in the absorption coefficient – smaller than 10^2 cm^{-1} (ZnSe and ZnS are completely transparent at 1.55 μm). Note that the

change in the refractive index increases with increasing the wavelength, and therefore such a large change can be achieved.

5. Conclusions

We have demonstrated the possibility of fabricating optical modulators based on ZnS/ZnSe heterostructures, which operate in the transparency region of materials, far from the excitation region. The operation in the transparency region reduces the absorption loss to minimum, while the location of the working range of the modulator far from the excitation wavelength and the energy band-gap edge eliminates the response delay caused by the recombination of carriers.

Such a unique combination of the properties of semiconductors and restrictions on the propagation of electromagnetic waves in photonic structures allows the fabrication of elements for optical devices with low thermal losses and signal attenuation. Silicon-based structures provide the integration of such modulators inside chips. The use of Bragg structures ensures a considerable reduction of the modulator size.

Acknowledgements. The authors thank A.G. Smirnov for placing the software for calculations of the reflection spectra of multilayer periodic structures at our disposal and for useful consultations. This work was supported by the Belarus Foundation for Basic Research and Russian Foundation for Basic Research.

References

1. Cotter D., Manning R.J., Blow K.J., Ellis A.D., Kelly A.E., Nesses D., Phillips I.D., Poustie A.J., Rogers D.C. *Science*, **286**, 19 (1999).
2. Liu Y.L., Liu E.K., Zhang S.L., Li G.Z., Luo J.S. *Electron. Lett.*, **30**, 2 (1994).
3. Zhao C.Z., Chen A.H., Liu E.K., Li G.Z. *IEEE Photonic Technol. Lett.*, **9**, 1113 (1997).
4. Montgomery R.G., Ghiron M., Gothoskar P., Patel V., Shastri K., Pathak S., Yanushevski K. US Patent 20040208454 (03.08.04).
5. Zhao C.Z., Li G.Z., Liu E.K., Gao Y., Liu X.D. *Appl. Phys. Lett.*, **67**, 17 (1995).
6. Treyz G.V., May P.G., Halbout J.-M. *Appl. Phys. Lett.*, **59**, 7 (1991).
7. Coppola G., Irace A., Iodice M., Cutolo A. *Opt. Eng.*, **40**, 6 (2001).
8. Stankevich V.V., Ermolenko M.V., Buganov O.V., Tikhomirov S.A., Gaponenko S.V., Kuznetsov P.I., Yakushcheva G.G. *Appl. Phys. B*, **81**, 257 (2005).
9. Ermolenko M.V., Tikhomirov S.A., Stankevich V.V., Buganov O.V., Gaponenko S.V., Kuznetsov P.I., Yakushcheva G.G. *Photon. Nanostr.: Fundam. Appl.*, **5**, 101 (2007).
10. Almeida V.R., Xu Q., Lipson M. *Opt. Lett.*, **30**, 18 (2005).
11. Liu A., Jones R., Liao L., Samara-Rubio D., Rubin D., Cohen O., Nicolaescu R., Pannicio M. *Nature*, **427**, 615 (2004).
12. Almeida V.R., Barrios C.A., Panepucci R.R., Lipson M., Foster M.A., Ouzounov D.G., Gaeta A.L. *Opt. Lett.*, **29**, 24 (2004).

13. Jacobsen R.S., Andersen K.N., Borel P.I., Fage-Pedersen J., Frandsen L.H., Hansen O., Kristensen M., Lavrinenko A.V., Moulin G., Ou H., Peucheret C., Zsigri B., Bjarklev A. *Nature*, **441**, 199 (2006).
14. Porte H., Hauden J., Mollier P., Grossard N., Jorge F., Lefevre R., Vuye S. *Techn. Dig. OFC/NFOEC* (Anaheim, CA, USA, 2005) Vol. 3.
15. Yang X., Mishra A.K., Lenstra D., Huijskens F.M., de Waardt H., Khoe G.D., Dorren H.J.S. *Opt. Commun.*, **236**, 329 (2004).
16. Asano T., Yoshizawa S., Noda S. *Appl. Phys. Lett.*, **29**, 27 (2001).
17. Pilipovich V.A., Esmen A.K., Goncharenko I.A., Kuleshov V.K. *Dokl. Nat. Acad. Sci. Belarus*, **48**, 6 (2004).
18. Kuznetsov P.I., Jytov V.A., Zakharov L.Yu., Shchamkhalova B.S., Korostelin Yu.V., Kozlovsky V.I. *Phys. Stat. Sol. (b)*, **229**, 171 (2002).
19. Blokhin A.P., Gelin M.F., Buganov O.V., Dubovskii V.A., Tikhomirov S.A., Tolstorozhev G.B. *Zh. Prikl. Spektrosk.*, **70**, 66 (2003).
20. Borisevich N.A., Buganov O.V., Tikhomirov S.A., Tolstorozhev G.B., Shred G.L. *Kvantovaya Elektron.*, **28**, 225 (1999) [*Quantum Electron.*, **29**, 780 (1999)].
21. Combescot M., Bok J. *J. Luminesc.*, **30**, 1 (1985).